Effect of Mechanical Loading on Electrical Conductivity in Human Intervertebral Disk

Alicia R. Jackson

Francesco Travascio

Wei Yong Gu[1]
e-mail: wgu@miami.edu

Department of Biomedical Engineering,
Tissue Biomechanics Laboratory,
University of Miami,
Coral Gables, FL 33146

The intervertebral disk (IVD), characterized as a charged, hydrated soft tissue, is the largest avascular structure in the body. Mechanical loading to the disk results in electromechanical transduction phenomenon as well as altered transport properties. Electrical conductivity is a material property of tissue depending on ion concentrations and diffusivities, which are in turn functions of tissue composition and structure. The aim of this study was to investigate the effect of mechanical loading on electrical behavior in human IVD tissues. We hypothesized that electrical conductivity in human IVD is strain-dependent, due to change in tissue composition caused by compression, and inhomogeneous, due to tissue structure and composition. We also hypothesized that conductivity in human annulus fibrosus (AF) is anisotropic, due to the layered structure of the tissue. Three lumbar IVDs were harvested from three human spines. From each disk, four AF specimens were prepared in each of the three principal directions (axial, circumferential, and radial), and four axial nucleus pulposus (NP) specimens were prepared. Conductivity was determined using a four-wire sense-current method and a custom-designed apparatus by measuring the resistance across the sample. Resistance measurements were taken at three levels of compression (0%, 10%, and 20%). Scanning electron microscopy (SEM) images of the human AF tissue were obtained in order to correlate tissue structure with conductivity results. Increasing compressive strain significantly decreased conductivity for all groups ($p<0.05$, analysis of variance (ANOVA)). Additionally, specimen orientation significantly affected electrical conductivity in the AF tissue, with conductivity in the radial direction being significantly lower than that in the axial or circumferential directions at all levels of compressive strain ($p<0.05$, ANOVA). Finally, conductivity in the NP tissue was significantly higher than that in the AF tissue ($p<0.05$, ANOVA). SEM images of the AF tissues showed evidence of microtubes orientated in the axial and circumferential directions, but not in the radial direction. This may suggest a relationship between tissue morphology and the anisotropic behavior of conductivity in the AF. The results of this investigation demonstrate that electrical conductivity in human IVD is strain-dependent and inhomogeneous, and that conductivity in the human AF tissue is anisotropic (i.e., direction-dependent). This anisotropic behavior is correlated with tissue structure shown in SEM images. This study provides important information regarding the effects of mechanical loading on solute transport and electrical behavior in IVD tissues. [DOI: 10.1115/1.3116152]

Keywords: annulus fibrosus, nucleus pulposus, anisotropy, compression, tissue mechanics, electrical behavior, morphology, scanning electron microscopy

1 Introduction

The intervertebral disk (IVD) of the spine plays a primarily mechanical role, supporting large compressive loads and allowing for spinal flexibility. The mechanical and transport properties of the disk are related to its unique composition and structure. The primary components of the IVD are water, proteoglycan (PG), and collagen [1,2]. The disk consists of the nucleus pulposus (NP), the annulus fibrosus (AF), and the cartilage end-plates; here, NP and AF tissues are investigated; see Fig. 1. The NP is composed of collagen fibrils arranged randomly in a proteoglycan gel, and is made up primarily of water (70–90%). The AF is formed by a series of concentric lamellae consisting of highly organized collagen fiber bundles [3,4].

Electrical conductivity, a material property of biological tissues, depends on ion concentrations and diffusivities within the tissue, which are functions of tissue composition and structure [5–11]. The conductivity of articular cartilage and animal IVD has been investigated [5–7,11–17]. Studies have shown that conductivity in cartilaginous tissues is sensitive to tissue hydration, but not to fixed charge density at physiological conditions [9,15]; conductivity has been linearly correlated with tissue hydration for animal IVD specimens with water content greater than 70% [14–16]. The dependence of conductivity on hydration is believed to be due to changes in ion diffusivities with tissue water content [11,14,15,17–19]. Our previous study demonstrated that conductivity in bovine IVD is anisotropic and inhomogeneous [17]. However, to our knowledge, no previous work has investigated the electrical conductivity of human IVD or the effect of mechanical loading on conductivity in IVD tissues.

Understanding how loading affects the transport and electrical properties of the IVD tissues is essential given the mechanical function of the disk. Mechanical loading of the disk results in an electromechanical transduction phenomenon, as well as altered solute transport [20]. Many studies have reported the effects of mechanical loading on water content, nutritional levels, and solute transport in IVD [1,21–30]. Because conductivity is closely related to ion diffusivities, further comprehension of the effects of loading on electrical behavior in IVD provides important insight into disk transport properties.

We hypothesized that the electrical conductivity of human IVD is strain-dependent due to changes in water content caused by tissue compression. We also hypothesized that, due to IVD composition and structure, conductivity is inhomogeneous within the disk, and anisotropic in AF due to its layered organization. Therefore, our objective was to measure the electrical conductivity of human AF and NP tissues under three levels of compressive strain, as well as that of AF in three major directions (axial, circumferential, and radial). The present study is essential in fully understanding the effect of mechanical loading on the electrical and transport behaviors in human IVD tissues.

2 Theoretical Background

Under zero fluid flow conditions, the electrical conductivity (χ) of a charged porous material is related to the intrinsic Na^+ and Cl^- ion diffusivities ($D^{+/-}$) by [10,11,13]

$$\chi = F_c^2 \phi^w (c^+ D^+ + c^- D^-)/RT \tag{1}$$

where F_c is the Faraday constant, ϕ^w is the tissue water volume fraction (or water content), R is the gas constant, T is the absolute

[1]Corresponding author. Also at Department of Biomedical Engineering, College of Engineering, University of Miami, P.O. Box 248294, Coral Gables, FL 33124-0621.

Contributed by the Bioengineering Division of ASME for publication in the JOURNAL OF BIOMECHANICAL ENGINEERING. Manuscript received August 22, 2008; final manuscript received December 11, 2008; published online April 13, 2009. Review conducted by Clark T. Hung.

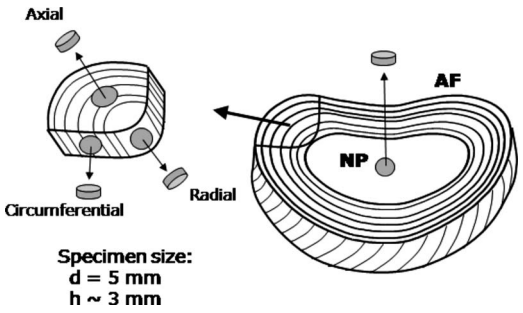

Fig. 1 Schematic of intervertebral disk showing sites and orientations of test specimens. AF indicates annulus fibrosus and NP indicates nucleus pulposus.

temperature, and c^+ and c^- are Na^+ and Cl^- ion concentrations, respectively. For negatively charged tissues, such as IVD, the ion concentrations in the tissue are related to the absolute value of the negative fixed charge density (FCD) (c^F) through the electroneutrality condition $c^+=c^-+c^F$ [31,32]. The ion concentrations within cartilaginous tissues can then be calculated based on the ideal Donnan equation. The value of the FCD within the tissue varies with tissue hydration by [33]

$$c^F = \frac{c_o^F(1-\phi^w)\phi_o^w}{(1-\phi_o^w)\phi^w} \tag{2}$$

where c_o^F and ϕ_o^w are the FCD and water volume fraction at a reference configuration. Thus, the ion concentrations (c^+ and c^-) within the tissue also vary with water content.

Recently, a new constitutive model was developed for the solute diffusivity (D^i, where superscript i stands for species) in tissue [16]

$$D^i = D_o^i \exp\left[-\alpha\left(\frac{r_s^i}{\sqrt{\kappa}}\right)^\beta\right] \tag{3}$$

where D_o^i and r_s^i are the solute diffusivity in an aqueous solution and solute Stokes' radius, respectively; κ is the Darcy permeability of the tissue; and α and β are the two positive parameters dependent on the structure of the porous media. For example, $\alpha=1.29\pm0.171$ and $\beta=0.372\pm0.088$ for porcine AF tissue [16]. The value of κ in Eq. (6) also varies with water content (ϕ^w) [34].

Since the water volume fraction of tissue (ϕ^w) is related to tissue dilatation e by

$$\phi^w = \frac{\phi_o^w + e}{1+e} \tag{4}$$

the ion concentrations and diffusivities are all strain-dependent.

3 Methods

3.1 Specimen Preparation. Three L3–L4 IVDs were harvested from three human lumbar spines (41-year-old male, 45-year-old female, and 45-year-old female, as Thompson grades I, II, and III, respectively). Disks were excised from spines, wrapped in plastic, and stored at −80°C. Cylindrical specimens (5 mm in diameter and ~3 mm thick) were prepared using a stainless steel corneal trephine (Biomedical Research Instruments, Inc., Silver Spring, MD) and sledge microtome (Model SM2400, Leica Instruments, Nussloch, Germany) with freezing stage (Model BFS-30, Physitemp Instruments Inc., Clifton, NJ). Four AF specimens were excised in each of the three principal directions (axial, circumferential, and radial), while four NP specimens were prepared in the axial direction only; see Fig. 1. Four groups of specimens were tested: three groups for the AF in each direction ($n=12$ for each group) and one group for NP ($n=12$). A total of three conductivity measurements, corresponding to three levels of compressive strain (0%, 10%, and 20%), were performed on each specimen.

3.2 Tissue Compression. Uniaxial confined compression of the tissue specimen was carried out in a separate compression chamber; see Fig. 2(*a*). The tissue was compressed between two porous plates in an acrylic chamber with an inner diameter of 5 mm. A separate compression chamber was used in order to avoid damage to Ag/AgCl electrodes in the conductivity chamber; see Fig. 2(*b*). Initially, the tissue was compressed by 20% inside the chamber and then quickly moved to the conductivity apparatus and confined to 20% strain for resistance measurement. Following measurement at 20% compression, the specimen was allowed to swell uniaxially to the height corresponding to 10% compression in a phosphate buffered saline (PBS) solution while confined in the conductivity chamber (5 mm in diameter; see Sec. 3.3). After measuring at 10% compression, the tissue was then allowed to swell back to its initial height (0% compression) and resistance was measured.

3.3 Conductivity Measurement. The apparatus used was similar to the one previously reported [14,15]. Briefly, it consists of two stainless steel current electrodes, two Teflon-coated Ag/AgCl voltage electrodes, a spacer, and a nonconductive acrylic chamber (Fig. 2(*b*)). A four-wire method was applied using a Keithley SourceMeter (Model 2400, Keithley Instruments Inc., Cleveland, OH). The resistance Ω across the tissue sample was measured at a low constant current of 10 μA. Electrical conductivity is related to resistance by

$$\chi = \frac{h}{\Omega \cdot A} \tag{5}$$

where A is the cross sectional area and h is the thickness of the sample. The distance between the electrodes and the height of the specimen could be controlled by the size of the spacers; see Fig.

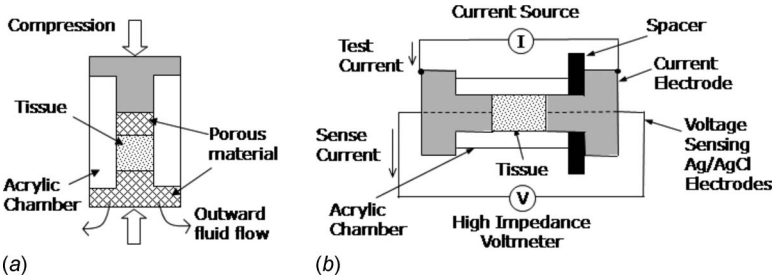

Fig. 2 Schematics of (*a*) compression apparatus and (*b*) apparatus for measuring strain-dependent electrical conductivity

2(*b*).

Conductivity measurements were taken at 20%, 10%, and 0% compression levels. For each level of strain, several resistance measurements were obtained at 10 min intervals to ensure the tissue had reached equilibrium following compression or swelling. Measurements were repeated until the same resistance value (within 5%) was measured for two consecutive readings, signifying equilibrium was reached (i.e., no fluid flow).

3.4 Measurement of Water Volume Fraction (or Water Content). The water volume fraction of specimens at the undeformed state (ϕ_o^w) was determined using a buoyancy method published in literature [14,15,35]. Briefly, the specimens were weighed in air (W_{air}) and in a PBS solution (W_{PBS}) using the density determination kit of a Sartorius analytical balance (Model LA120S, Goettingen, Germany); specimens were then lyophilized and weighed to determine the dry weight (W_{dry}). The water volume fraction was calculated by

$$\phi_o^w = \frac{(W_{\text{wet}} - W_{\text{dry}})}{(W_{\text{wet}} - W_{\text{PBS}})} \frac{\rho_{\text{PBS}}}{\rho_w} \tag{6}$$

where ρ_{PBS} and ρ_w are the densities of PBS and water, respectively. The water volume fraction of tissue at different compression levels (ϕ^w) could be calculated by Eq. (4).

3.5 Scanning Electron Microscopy. Scanning electron microscopy (SEM) images were obtained in order to compare conductivity trends with tissue structure. The images of the axial, radial, and circumferential sections of the anterior region of the human L3–L4 AF were acquired. Samples were fixed with a 2% gluteraldehyde (Electron Microscopy Sciences, Hatfield, PA) in PBS, dehydrated in ethanol, and dried by immersion in hexamethyldisilizane (Electron Microscopy Sciences, Hatfield, PA) [36]. After sputter coating with Pd (Sputter Coater 108auto, Cressington, Watford, UK), high-resolution SEM images were obtained by a scanning electron microscope (XL30 ESEM-FEG, FEI Co., Hillsborg, OR) operating in a high-vacuum mode.

3.6 Statistical Analysis. To investigate the effect of compression and direction on conductivity in human AF specimens, a two-way ANOVA was performed using SPSS software (SPSS Inc., Chicago, IL). The two factors were direction (three levels: axial, circumferential, and radial) and level of compression (three levels: 0%, 10%, and 20%). For human NP specimens, a one-way ANOVA was performed using SPSS software with level of compression being the factor (three levels: 0%, 10%, and 20%). The Student–Newman–Keuls post hoc test was used for ANOVA analysis using SPSS software in order to determine between which levels of each factor the differences were significant. A Student t-test was performed to compare conductivity values for NP and each group of AF specimens. For all tests, the significance level was set at $p < 0.05$.

4 Results

The results for electrical conductivity measurements at 21.5°C are shown in Fig. 3. Values for water content at reference configuration (i.e., 0% compression) and under compression are shown in Table 1. Electrical conductivity in the NP specimens was significantly higher than that in the AF specimens for all tissue orientations at all levels of compressive strain ($p < 0.05$). For both AF and NP specimens, there was a significant decrease in electrical conductivity with increasing compressive strain ($p < 0.05$). Furthermore, in the AF tissue, specimen orientation was shown to have a significant effect on electrical conductivity, with values in the radial direction being significantly lower than those in the axial or circumferential directions ($p < 0.05$).

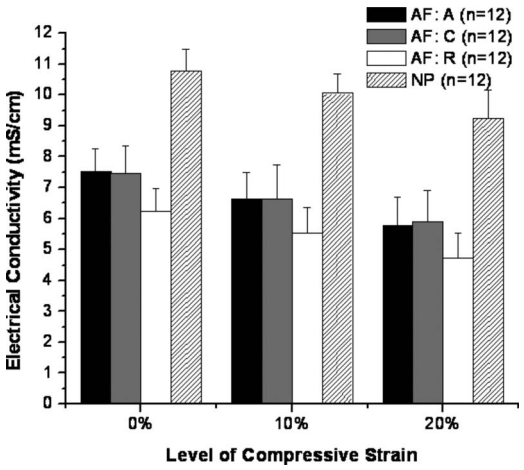

Fig. 3 Variation of electrical conductivity with increasing compressive strain for AF and NP tissues. For the AF tissue, the results for conductivity in three directions are shown: axial (A), circumferential (C), and radial (R). Variation bars signify standard deviation (SD). Statistical analysis showed a significant difference ($p < 0.05$) between conductivity values for all groups except axial AF and circumferential AF (at all levels of compressive strain).

5 Discussion

The objective of this study was to determine the effect of mechanical strain on electrical conductivity in human IVD as well as the anisotropic trend for conductivity in human AF. Our results for conductivity in human IVD are comparable with previously reported values of conductivity in a human articular cartilage (6–10 mS/cm) [9,11]. The results also indicate that electrical conductivity in human IVD is dependent on tissue composition and structure.

The significant decrease in conductivity with increased loading indicates that electrical conductivity in human IVD is strain-dependent. To our knowledge, this is the first study showing this behavior for human IVD. The decrease in conductivity with increasing strain is mainly due to water content reduction caused by increasing compression; see Eq. (4). Previous studies have shown that electrical conductivity increases with increasing tissue hydration [14–16], which is attributed to an increase in ion diffusivities with increasing tissue hydration [11,14,15,17–19]. Tissue compression causes fluid exudation and a corresponding decrease in tissue water content. This results in decreased ion diffusivity in the tissue and subsequent decreased electrical conductivity. Similar strain-dependent behavior was found for glucose and oxygen diffusivity in bovine AF [29,30] and water diffusivity in IVD tis-

Table 1 Water volume fraction for IVD tissue specimens at three levels of compression. The values at the reference configuration (i.e., compression=0%) were measured using buoyancy method. Values for the water volume fraction of compressed (10% and 20%) tissue were calculated from Eq. (4) using ϕ_o^w. The values are expressed in mean±SD. For all groups, n=12.

	ϕ_o^w (0%)	ϕ^w (10%)	ϕ^w (20%)
Axial AF	0.80 ± 0.02	0.78 ± 0.02	0.75 ± 0.03
Radial AF	0.79 ± 0.04	0.77 ± 0.05	0.74 ± 0.05
Circumferential AF	0.79 ± 0.02	0.77 ± 0.03	0.74 ± 0.03
Axial NP	0.86 ± 0.02	0.85 ± 0.03	0.83 ± 0.03

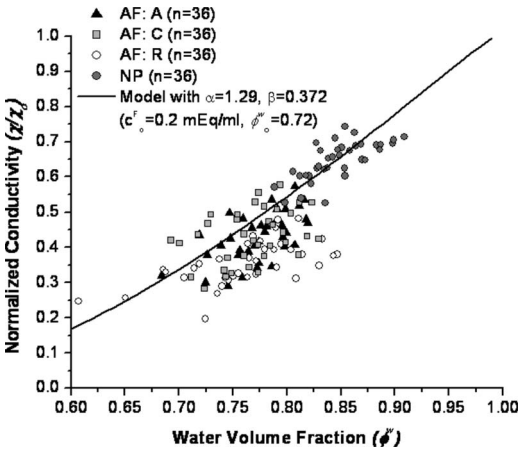

Fig. 4 Model prediction of normalized conductivity in human AF and NP tissues compared with experimental data. The value of FCD was assumed to be 0.2 mEq/ml at water volume fraction of 0.72. The values for α and β were taken from literature [16].

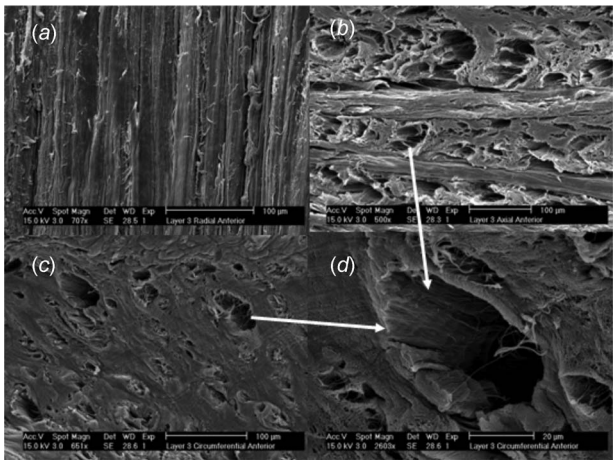

Fig. 5 SEM images showing obviously (*a*) no obviously visible microtubes in the radial section of human AF, (*b*) the clear presence of microtubes in the axial and (*c*) circumferential sections, and (*d*) a magnified view of the microtube

sue [27,28]. Our results also qualitatively agree with the theoretical prediction of monotonically decreasing conductivity with increasing tissue compression [5,13].

Our theoretical model, shown in Eq. (3), could quantitatively predict the experimental results for strain-dependent electrical conductivity, Fig. 4. Note that in Fig. 4, the conductivity (χ) is normalized by the conductivity of bathing solution (χ_o). The averaged FCD of the IVD specimens was estimated to be $c_o^F = 0.20$ mEq ml^{-1} at the corresponding water volume fraction of $\phi_o^w = 0.72$, based on the results for human IVD found in literature [37]. Ion diffusivities were calculated from Eq. (3), using $\alpha = 1.29$ and $\beta = 0.372$, as well as our previous model for hydraulic permeability [16,33]. Note that these values were determined for porcine AF tissue with axial orientation; values are not known for human AF and NP tissues. The values for Stokes' radii and ion diffusivity in water for Na^+ and Cl^- ions were obtained from literature [16,38]. The model reasonably predicts a strain-dependent conductivity behavior in human IVD tissues, as is shown in Fig. 4, although it appears to overestimate conductivity values for radial AF, indicating that the material parameters (α and β) for axial AF would be different from those for radial AF (i.e., anisotropy). Nonetheless, it is evident that the model is capable of predicting a strain-dependent conductivity behavior in human IVD tissues. It is likely that prediction accuracy would be greatly improved if the values for α and β for human NP and AF tissues are determined for each of the three major orientations (axial, circumferential, and radial).

Our findings also indicate that the electrical conductivity in the human AF tissue is anisotropic, i.e., direction-dependent. To our knowledge, this is the first study reporting the anisotropic behavior of electrical conductivity in human IVD. Conductivity in the radial direction was significantly lower than that in the axial or circumferential directions for all levels of compression. This is in agreement with previous findings for electrical conductivity in bovine AF [17], as well as with findings for the diffusion coefficient of water [27,39], glucose [29], and fluorescein in IVD [40].

To further investigate the anisotropy of electrical conductivity and its related ion diffusivity, AF structure was studied using SEM and compared with the trends found in conductivity results (Fig. 5). The SEM images of the axial and circumferential specimens in Figs. 5(*b*)–5(*d*) distinctly show microtubes running parallel to the collagen fiber bundles, while microtubes are not obviously visible in the radial specimen image shown in Fig. 5(*a*). Several previous studies have presented SEM images showing a similar microtube structure in a rat tail IVD [41] and in a bovine tail IVD [29,40]. The presence of microtubes may provide explanation for the anisotropic behavior of electrical conductivity in AF. It is possible that the organization of these microtubes along collagen fibers may provide a preferred pathway of transport in the axial and circumferential directions; on the other hand, because the microtubes do not appear to be contiguous between adjacent lamellae, no such direct path appears to exist in the radial direction.

The significant difference between conductivity values in NP as compared with those in AF indicates that electrical conductivity in human IVD is inhomogeneous. The regional variation results from the distinct composition and structure of AF and NP tissues; compositional differences are evidenced by the variation in tissue water content (Table 1). These findings are in agreement with our previous study demonstrating the inhomogeneous behavior of electrical conductivity in a bovine IVD [17].

In summary, the effect of mechanical compression on the electrical behavior in human IVD tissues was investigated by measuring strain-dependent electrical conductivity. Our results indicate the conductivity in human IVD depends on both tissue composition, i.e., water content and structure. It was determined that electrical conductivity in human IVD is strain-dependent due to tissue compositional changes (i.e., decreased water content) caused by compression. Furthermore, we also determined that conductivity in human IVD is inhomogeneous, with that in the NP tissue being higher than the AF tissue. Finally, it was found that electrical conductivity in the human AF is anisotropic, most likely due to the microtube structure of the tissue. The results of this investigation are important in further understanding the transport properties and nutritional pathways in IVD, as well as the mechanical-to-electrical transduction phenomena in IVD tissues.

Acknowledgment

This project was supported by a grant from the NIH NIAMS (Grant No. AR50609). The authors also wish to thank Mr. Larry Hazbun and Mr. Andre Castillo for their assistance in apparatus machining.

References

[1] Kraemer, J., Kolditz, D., and Gowin, R., 1985, "Water and Electrolyte Content of Human Intervertebral Discs Under Variable Load," Spine, **10**(1), pp. 69–71.
[2] Urban, J. P. G., and Maroudas, A., 1980, "The Chemistry of the Intervertebral Disc in Relation to Its Physiological Function and Requirements," Clin. Rheum. Dis., **6**, pp. 51–77.
[3] Hickey, D. S., and Hukins, D. W. L., 1980, "Relation Between the Structure of the Anulus Fibrosus and the Function and Failure of the Intervertebral Disc," Spine, **5**(2), pp. 106–116.

[4] Marchand, F., and Ahmed, A. M., 1990, "Investigation of the Laminate Structure of Lumbar Disc Anulus Fibrosus," Spine, **15**(5), pp. 402–410.
[5] Chammas, P., Federspiel, W. J., and Eisenberg, S. R., 1994, "A Microcontinuum Model of Electrokinetic Coupling in the Extracellular Matrix: Perturbation Formulation and Solution," J. Colloid Interface Sci., **168**, pp. 526–538.
[6] Eisenberg, S. R., and Grodzinsky, A. J., 1988, "Electrokinetic Micromodel of Extracellular-Matrix and Other Poly-Electrolyte Networks," PCH, Physico-Chem. Hydrodyn., **10**(4), pp. 517–539.
[7] Grodzinsky, A. J., 1983, "Electromechanical and Physicochemical Properties of Connective Tissue," Crit. Rev. Biomed. Eng., **9**(2), pp. 133–199.
[8] Gu, W. Y., Lai, W. M., and Mow, V. C., 1998, "A Mixture Theory for Charged-Hydrated Soft Tissues Containing Multi-Electrolytes: Passive Transport and Swelling Behaviors," ASME J. Biomech. Eng., **120**(2), pp. 169–180.
[9] Hasegawa, I., Kuriki, S., Matsuno, S., and Matsumoto, G., 1983, "Dependence of Electrical Conductivity on Fixed Charge Density in Articular Cartilage," Clin. Orthop. Relat. Res., **177**, pp. 283–288.
[10] Helfferich, F., 1962, *Ion Exchange*, McGraw-Hill, New York.
[11] Maroudas, A., 1968, "Physicochemical Properties of Cartilage in the Light of Ion Exchange Theory," Biophys. J., **8**(5), pp. 575–595.
[12] Chammas, P., 1989, "Electromechanical Coupling in Articular Cartilage: An Electromechanical Micromodel and Experimental Results," MS thesis, Boston University, Boston, MA.
[13] Frank, E. H., Grodzinsky, A. J., Phillips, S. L., and Grimshaw, P. E., 1990, "Physiochemical and Bioelectrical Determinants of Cartilage Material Properties," *Biomechanics of Diarthrodial Joints*, V. C. Mow, D. O. Wood, S. L. Woo, eds., Springer, New York, pp. 261–282.
[14] Gu, W. Y., and Justiz, M. A., 2002, "Apparatus for Measuring the Swelling Dependent Electrical Conductivity of Charged Hydrated Soft Tissues," ASME J. Biomech. Eng., **124**, pp. 790–793.
[15] Gu, W. Y., Justiz, M. A., and Yao, H., 2002, "Electrical Conductivity of Lumbar Annulus Fibrosis: Effects of Porosity and Fixed Charge Density," Spine, **27**, pp. 2390–2395.
[16] Gu, W. Y., Yao, H., Vega, A. L., and Flagler, D., 2004, "Diffusivity of Ions in Agarose Gels and Intervertebral Disc: Effect of Porosity," Ann. Biomed. Eng., **32**, pp. 1710–1717.
[17] Jackson, A. R., Yao, H., Brown, M. D., and Gu, W. Y., 2006, "Anisotropic Ion Diffusivity in Intervertebral Disc: An Electrical Conductivity Approach," Spine, **31**(24), pp. 2783–2789.
[18] Schepps, J. L., and Foster, K. R., 1980, "The UHF and Microwave Dielectric Properties of Normal and Tumour Tissues: Variation in Dielectric Properties With Tissue Water Content," Phys. Med. Biol., **25**(6), pp. 1149–1159.
[19] Mackie, J. S., and Meares, P., 1955, "The Diffusion of Electrolytes in a Cation-Exchange Resin. I. Theoretical," Proc. R. Soc. London, Ser. A, **232**, pp. 498–509.
[20] Setton, L. A., and Chen, J., 2006, "Mechanobiology of the Intervertebral Disc and Relevance to Disc Degeneration," J. Bone Jt. Surg., Am. Vol., **88**(Suppl. 2), pp. 52–57.
[21] Holm, S., and Nachemson, A., 1982, "Nutritional Changes in the Canine Intervertebral Disc After Spinal Fusion," Clin. Orthop. Relat. Res., **169**, pp. 243–258.
[22] Bibby, S. R., Fairbank, J. C., Urban, M. R., and Urban, J. P., 2002, "Cell Viability in Scoliotic Discs in Relation to Disc Deformity and Nutrient Levels," Spine, **27**(20), pp. 2220–2228.
[23] Adams, M. A., and Hutton, W. C., 1986, "The Effect of Posture on Diffusion Into Lumbar Intervertebral Discs," J. Anat., **147**, pp. 121–134.
[24] Ohshima, H., Tsuji, H., Hiarano, N., Ishihara, H., Katoh, Y., and Yamada, H., 1989, "Water Diffusion Pathway, Swelling Pressure, and Biomechanical Properties of the Intervertebral Disc During Compression Load," Spine, **14**(11), pp. 1234–1244.
[25] Adams, M. A., and Hutton, W. C., 1983, "The Effect of Posture on the Fluid Content of Lumbar Intervertebral Discs," Spine, **8**(6), pp. 665–671.
[26] Terahata, N., Ishihara, H., Ohshima, H., Hirano, N., and Tsuji, H., 1994, "Effects of Axial Traction Stress on Solute Transport and Proteoglycan Synthesis in the Porcine Intervertebral Disc In Vitro," Eur. Spine J., **3**(6), pp. 325–330.
[27] Chiu, E. J., Newitt, D. C., Segal, M. R., Hu, S. S., Lotz, J. C., and Majumdar, S., 2001, "Magnetic Resonance Imaging Measurement of Relaxation and Water Diffusion in the Human Lumbar Intervertebral Disc Under Compression In Vitro," Spine, **26**(19), pp. E437–E444.
[28] Drew, S. C., Silva, P., Crozier, S., and Pearcy, M. J., 2004, "A Diffusion and T2 Relaxation MRI Study of the Ovine Lumbar Intervertebral Disc Under Compression In Vitro," Phys. Med. Biol., **49**(16), pp. 3585–3592.
[29] Jackson, A. R., Yuan, T.-Y., Huang, C.-Y., Travascio, F., and Gu, W. Y., 2008, "Effect of Compression and Anisotropy on the Diffusion of Glucose in Annulus Fibrosus," Spine, **33**(1), pp. 1–7.
[30] Yuan, T.-Y., Jackson, A. R., Huang, C.-Y., and Gu, W. Y., 2008, "Strain-Dependent Oxygen Diffusivity in Bovine Annulus Fibrosus," Proceedings of the ASME Summer Bioengineering Conference, SBC2008, p. 192842.
[31] Katchalsky, A., and Curran, P. F., 1975, *Nonequilibrium Thermodynamics in Biophysics*, Harvard University Press, Cambridge, MA.
[32] Lai, W. M., Hou, J. S., and Mow, V. C., 1991, "A Triphasic Theory for the Swelling and Deformation Behaviors of Articular Cartilage," ASME J. Biomech. Eng., **113**(3), pp. 245–258.
[33] Gu, W. Y., and Yao, H., 2003, "Effects of Hydration and Fixed Charge Density on Fluid Transport in Charged Hydrated Soft Tissue," Ann. Biomed. Eng., **31**(10), pp. 1162–1170.
[34] Gu, W. Y., Yao, H., Huang, C.-Y., and Cheung, H. S., 2003, "New Insight Into Deformation-Dependent Hydraulic Permeability of Gels and Cartilage, and Dynamic Behavior of Agarose Gels in Confined Compression," J. Biomech., **36**, pp. 593–598.
[35] Yao, H., Justiz, M. A., Flagler, D., and Gu, W. Y., 2002, "Effects of Swelling Pressure and Hydraulic Permeability on Dynamic Compressive Behavior of Lumbar Annulus Fibrosus," Ann. Biomed. Eng., **30**, pp. 1234–1241.
[36] Hayat, M. A., 1982, *Fixation for Electron Microscope*, Academic Press, New York, NY, p. 501.
[37] Iatridis, J. C., MacLean, J. J., O'Brien, M., and Stokes, I. A. F., 2007, "Measurements of Proteoglycan and Water Content Distribution in Human Lumbar Intervertebral Discs," Spine, **32**(14), pp. 1493–1497.
[38] Koneshan, S., Rasaiah, J. C., Lynden-Bell, R. M., and Lee, S. H., 1998, "Solvent Structure, Dynamics, and Ion Mobility in Aqueous Solution at 25°C," J. Phys. Chem., **102**, pp. 4193–4204.
[39] Hsu, E. W., and Setton, L. A., 1999, "Diffusion Tensor Microscopy of the Intervertebral Disc Anulus Fibrosus," Magn. Reson. Med., **41**(5), pp. 992–999.
[40] Travascio, F., and Gu, W., 2007, "Anisotropic Diffusive Transport in Annulus Fibrosus: Experimental Determination of the Diffusion Tensor by FRAP Technique," Ann. Biomed. Eng., **35**(10), pp. 1739–1748.
[41] Iatridis, J. C., and ap Gwynn, I., 2004, "Mechanisms for Mechanical Damage in the Intervertebral Disc Annulus Fibrosus," J. Biomech., **37**, pp. 1165–1175.